Fundamental Study of Driving Force Distribution Method for Minimization of Maximum Slip Ratio for Electric Vehicles with In-wheel Motors

Naoto Shimoya[1)] **Hiroshi Fujimoto**[1)]

1) The University of Tokyo, 5-1-5 Kashiwanoha, Kashiwa, Chiba, 277-8561 Japan
(E-mail: shimoya15@hflab.k.u-tokyo.ac.jp)

Presented at the EVTeC and APE Japan on May 25, 2016

ABSTRACT: Aiming at minimizing the slip ratio and guaranteeing the total driving force with low calculation cost, this paper presents a novel driving force distribution method for four-wheel-driven electric vehicles. By using the property of the infinity norm which is called Equal Magnitude Property (EMP), vehicle safety can be improved in comparison with conventional methods. The effectiveness of the proposed method is verified by simulations and experiments.

KEY WORDS: electric vehicle, slip ratio, driving stiffness, infinity norm, equal magnitude property

1. INTRODUCTION

Facing environmental and energy problems, Electric Vehicles (EVs) have attracted attention in recent years. EVs have great advantages in terms of motion control compared with Internal Combustion Engine Vehicles (ICEVs)[(1)].

(a) The torque response of electric motors is 100-500 times faster than that of engines.

(b) All wheels can be controlled independently by adopting small high-power in-wheel motors.

(c) The output torque of an electric motor can be measured accurately from the motor current.

Based on these advantages, many traction control and motion stabilization methods have been proposed[(2)(3)(4)]. The authors' group proposed driving force control method (DFC)[(2)] based on traction and slip ratio control. DFC is a control method that controls driving force references to keep the wheels working in the unsaturated region. With this method, a driver can drive safely and comfortably. Moreover, by distributing and compensating driving force among the four wheels, the slip ratios can be suppressed and the total driving force can follow the reference value.

There are two methods for driving force distribution. One is using the tire workload[(5)(6)], but as it regards friction coefficient μ as known, a momentary estimation method of the road condition is required. the second one is using the slip ratio[(7)]. As slip ratio can be calculated in real time, it is suitable to use in driving force distribution algorithms.

If one of the wheels slip, vehicle stability may become unstable. Therefore, driving force distribution algorithm which minimize maximum slip ratio of wheels is necessary for vehicle stability. Some previous studies are provided as bellows.

Computed method[(5)] enables finding a optimal solution, but the calculation cost is heavy. In (6)(7), a method that minimizing the sum of squares of slip ratios is proposed. Although this method is computational cheap, it minimizes 2-norm, which is the mean value of all slip ratios, not infinity-norm, i.e., the solution is not optimal for traction control.

In this study, to minimize the maximum slip ratio, a method using the property of infinity-norm, also known as Equal Magnitude Property (EMP)[(8)(9)], is employed. This method is expected to find solution of minimizing maximum slip ratio with small calculation cost. In this paper, As a Basic study of driving force distribution method using EMP, driving force distribution minimizing maximum slip ratio in acceleration is investigated. The effectiveness of the proposed method is verified by simulations and experiments.

Fig. 1: FPEV2-Kanon.

Table 1: Vehicle specification.

Vehicle mass M	871 kg
Wheel base l_f	0.999 m
Wheel base l_r	0.701 m
Gravity height h_g	0.51 m
Wheel radius r	0.302 m
Vehicle inertia I	617 kgm^2
Tread width d_i	1.3 m

2. EXPERIMENTAL VEHICLE AND VEHICLE MODEL

2.1. Experimental Vehicle

The experimental EV "FPEV2-Kanon", developed by the authors' laboratory, is shown in Fig. 1. Outer-rotor-type in-wheel motors are installed in each wheel and these motors adopt direct drive system. The maximum torque of each of the front motors is $\pm$500 Nm, and that of the rear is $\pm$530 Nm. Table 1 presents

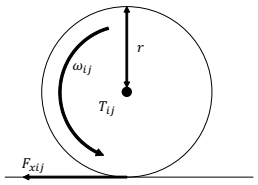

Fig. 2: Wheel model.

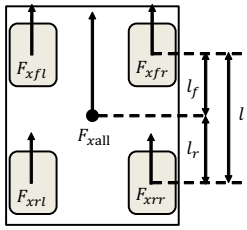

Fig. 3: Vehicle model.

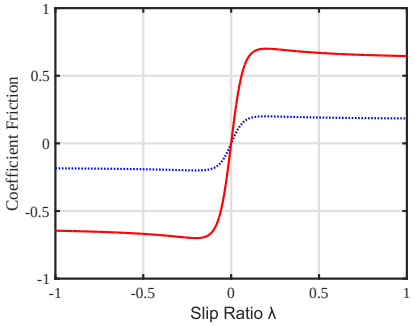

Fig. 4: $\mu - \lambda$ relationship.

other specifications.

2.2. Vehicle Model

In this section, A four independent wheel driven EV is modeled. The equations of wheel rotation and vehicle dynamics considered only straight driven as shown in Fig. 2, 3 are written as follows.

$$J_i \dot{\omega}_{ij} = T_{ij} - rF_{xij} \tag{1}$$

$$F_{x\mathrm{all}} = F_{xfl} + F_{xfr} + F_{xrl} + F_{xrr} \tag{2}$$

$$M_z = -\frac{d_f}{2}F_{xfl} + \frac{d_f}{2}F_{xfr} - \frac{d_r}{2}F_{xrl} + \frac{d_r}{2}F_{xrr} \tag{3}$$

where J_i is the wheel inertia, ω_{ij} is the wheel angular velocity, T_{ij} is the motor torque, r is the wheel radius, F_{xij} is the driving force, $F_{x\mathrm{all}}$ is the total driving force and d_i is tread base. Also, the subscript i represents f or r (f is front and r is rear) and j represents l or r (l is left and r is right).

When the vehicle accelerates or decelerates, the wheel velocity $V_\omega = r\omega$ differs from the vehicle velocity V because of tires' elastic deformation. Therefore the slip ratio λ_{ij} is defined as follow.

$$\lambda_{ij} = \frac{V_{\omega_{ij}} - V}{\max(V_{\omega_{ij}}, V, \epsilon)} \tag{4}$$

where ϵ is a tiny value to prevent division by zero.

The driving force F_{xij} and the driving stiffness D_{sij} at each wheel are obtained as follows.

$$F_{xij} = \mu_{ij} F_{zij} \tag{5}$$

$$D_{sij} = \left.\frac{dF_{xij}}{d\lambda_{ij}}\right|_{\lambda_{ij}=0} \tag{6}$$

where F_{zij} is the normal reaction force on each wheel, and μ_{ij} is the friction coefficient.

The $\mu - \lambda$ relationship which depends on the road condition is shown in Fig. 4[10]. There are $\lambda_{\mathrm{peak,p}}, \lambda_{\mathrm{peak,n}}$ which μ is the maximum or the minimum. In the range of $\lambda_{\mathrm{peak,n}} \leq \lambda_{ij} \leq \lambda_{\mathrm{peak,p}}$, μ is approximated by a monotonically increasing function of λ, and outside the range, a monotonically decreasing function because of μ saturation.

3. TRACTION CONTROL

3.1. Driving Force Control[2]

In this section, the driving force control (DFC) method is explained[2].

The block diagram of DFC is shown in Fig. 5, The outer loop is a driving force loop and the inner loop is a wheel velocity loop that controls the slip ratio. From the (1), the driving force of each wheel is estimated by Driving Force Observer (DFO) as a disturbance of motor torque command ${T_{ij}}^*$ and wheel velocity ω_{ij}. Here, $\hat{F}_{xij}$ is the driving force reference and ${F_{xij}}^*$ is the estimated driving force.

Since the definition of slip ratio λ_{ij} for acceleration ($V_{\omega_{ij}} \geq V$) differs from the definition for deceleration ($V_{\omega_{ij}} < V$), λ_{ij} is inconvenient to control. Therefore, instead of the slip ratio, the control input y_{ij}, defined as follows, is controlled.

$$y_{ij} = \frac{V_{\omega_{ij}}}{V} - 1 \tag{7}$$

This is the same definition as the definition of slip ratio for deceleration. The relationship between λ_{ij} and y_{ij} for acceleration is calculated as

$$y_{ij} = \frac{\lambda_{ij}}{1 - \lambda_{ij}} \tag{8}$$

y_{ij} approximately equals to λ_{ij} when $\mid \lambda_{ij} \mid \ll 1$ and they are always one to one correspondence.

From (7), the wheel velocity reference ${V_{\omega_{ij}}}^*$ of the inner loop is calculated as

$${V_{\omega_{ij}}}^* = (1 + y_{ij})V \tag{9}$$

which shows that the vehicle can not start moving when it stops ($V = 0$) since ${V_{\omega_{ij}}}^*$ is equal to zero independent of y_{ij}. To prevent this problem, the reference ${V_{\omega_{ij}}}^*$ is modified where V is smaller than a given constant σ as shown in (10).

$$\begin{cases} {V_{\omega_{ij}}}^* = V + y_{ij}\sigma & (V < \sigma) \\ {V_{\omega_{ij}}}^* = V + y_{ij}V & (V \geq \sigma) \end{cases} \tag{10}$$

From (6), it can be considered that $F_{xij} = D_{sij}\lambda_{ij}$ provided that $\mid \lambda_{ij} \mid \ll 1$. In addition, assuming that wheel velocity control is enough fast to satisfy $y_{ij} = \lambda_{ij}$, the transfer function from y_{ij} to F_{xij} is assumed to be zero order as

$$F_{xij} = D_{sij}\lambda_{ij} \simeq D_{sij}y_{ij} \tag{11}$$

Therefore, the driving force controller is set as I control with gain K_I, and the initial value is set as $y_{ij0} = 0$ by assuming that the vehicle is in non-driving condition. By defining the upper limit $y_{ij\max}$ and the lower limit $y_{ij\min}$ for the integrator, saturation is applied the integrator output for limiting y to $y_{ij\min} \leq y_{ij} \leq y_{ij\max}$. With this saturation, traction can be retained by keeping the slip ratio within the range where μ is monotonic function of λ.

3.2. Slip Ratio Estimation[11]

The slip ratio estimation is applied to obtain the longitudinal acceleration a_x and the wheel velocity ω_{ij} with vehicle-mounted sensors.

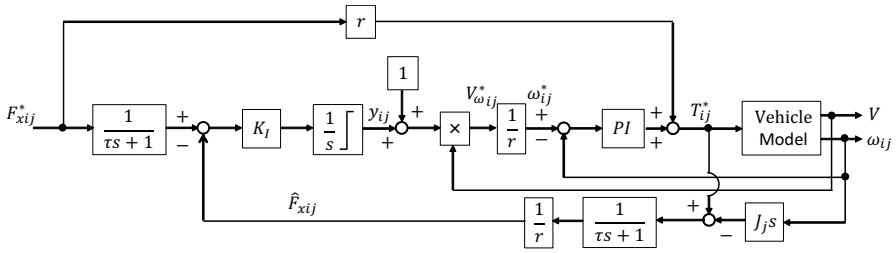

Fig. 5: Driving Force Control (DFC).

To differentiate both sides in (4), state equation of λ_{ij} is calculated as

$$\dot{\hat{\lambda}}_{ij} = \frac{\dot{\omega}_{ij}}{\omega_{ij}}(1+\hat{\lambda}_{ij}) - \frac{a_x}{r^2\omega_{ij}}(1+\hat{\lambda}_{ij})^2 \tag{12}$$

From (4), V_{ij} is estimated as (13), and let the vehicle velocity$V$ be the average of each wheel velocity V_{ij}.

$$V_{ij} = \frac{r\omega_{ij}}{1+\hat{\lambda}_{ij}} \tag{13}$$

3.3. Driving Stiffness Estimation[7]

From (11), since the relationship between F_{xij} and λ_{ij} is $F_{xij} = D_{sij}\lambda_{ij}$ provided that $|\ \lambda_{ij}\ | \ll 1$, a Recursive Least Squares (RLS) Method is available. Therefore, $\hat{D}_{sij}$ can be estimated by $\hat{F}_{xij}$, $\hat{\lambda}_{ij}$ and a forgetting coefficient w. $\hat{D}_{sij}$ at a sample point k is estimated as follows.

$$\hat{D}_{sij}(k) = \hat{D}_{sij}(k-1) - \frac{\Gamma(k-1)\hat{\lambda}_{ij}(k)}{w+\hat{\lambda}_{ij}(k)\Gamma(k-1)\hat{\lambda}_{ij}(k)} \times[\hat{\lambda}_{ij}\hat{D}_{sij}(k-1) - \hat{F}_{xij}(k)] \tag{14}$$

$$\Gamma(k) = \frac{1}{w}\left[\Gamma(k-1) - \frac{\Gamma(k-1)\hat{\lambda}^2_{ij}(k)\Gamma(k-1)}{w+\hat{\lambda}_{ij}(k)\Gamma(k-1)\hat{\lambda}_{ij}(k)}\right] \tag{15}$$

If $\lambda_{ij}(k)$ is about zero, $\hat{\lambda}_{ij}$ becomes very small and reliability of $\hat{D}_{sij}$ is decreased. Therefore $\hat{D}_{ij}(k)$ and $\Gamma(k)$ are not updated if $|\ \lambda_{ij}(k)\ | < 0.005$. Lower limitations 1000 are imposed to $\hat{D}_{ij}(k)$ avoiding division by zero.

3.4. Driving Force Distribution Method based on Sum of squares minimization (conventional)[7]

When the slip ratio λ_{ij} increases on a slippery road and reaches idling region, driving force is saturated and reduced. To avoid this reduction, total driving force reference ${F_{x\mathrm{all}}}^*$ has to be distributed appropriately so that λ_{ij} of each wheel is small enough to prevent saturation. Therefore, driving force distribution method should decide the driving force reference ${F_{xij}}^*$ of each wheel to minimize λ_{ij} of each wheel, satisfying total driving force reference ${F_{x\mathrm{all}}}^*$ and yaw-moment reference ${M_z}^*$ generated by driving force difference between left and right.

The relationship between driving force of each wheel F_{xij} and $F_{x\mathrm{all}}$, M_z is as follow:

$$\begin{bmatrix} 1 & 1 & 1 & 1 \\ -\frac{d_f}{2} & \frac{d_f}{2} & -\frac{d_r}{2} & \frac{d_r}{2} \end{bmatrix} \begin{bmatrix} F_{xfl} \\ F_{xfr} \\ F_{xrl} \\ F_{xrr} \end{bmatrix} = \begin{bmatrix} F_{x\mathrm{all}} \\ M_z \end{bmatrix} \tag{16}$$

Here, by setting the coefficient matrix in the left-hand side as $\boldsymbol{A}$, the vector of driving force of each wheel $[F_{xfl}, F_{xfr}, F_{xrl}, F_{xrr}]^T$ as $\boldsymbol{x}$, and total driving force and yaw-moment $[F_{x\mathrm{all}}, M_z]^T$ as $\boldsymbol{b}$, (16) can be rewritten as $\boldsymbol{Ax} = \boldsymbol{b}$.

From (11), slip ratio of each wheel λ_{ij} in the range of $|\lambda_{ij}| \ll 1$ can be obtained as

$$\lambda_{ij} = \frac{F_{xij}}{D_{sij}} \tag{17}$$

Then the cost function J is defined as the sum of squares of slip ratio λ_{ij} .

$$\begin{aligned} J &= \sum_{i=f,r}\sum_{j=l,r}(\lambda_{ij})^2 \\ &= \frac{{F_{xfl}}^2}{{D_{sfl}}^2} + \frac{{F_{xfr}}^2}{{D_{sfr}}^2} + \frac{{F_{xrl}}^2}{{D_{srl}}^2} + \frac{{F_{xrr}}^2}{{D_{srr}}^2} \\ &= \boldsymbol{x}^T\boldsymbol{W}\boldsymbol{x} \end{aligned} \tag{18}$$

The weighted least squares solution $\boldsymbol{x}_{\mathbf{opt}}$ of (18) that minimizes J, and weighting matrix $\boldsymbol{W}$ are as follows.

$$\boldsymbol{x}_{\mathbf{opt}} = \boldsymbol{W}^{-1}\boldsymbol{A}^T(\boldsymbol{A}\boldsymbol{W}^{-1}\boldsymbol{A}^T)^{-1}\boldsymbol{b} \tag{19}$$

$$\boldsymbol{W} = \mathrm{diag}\left(\frac{1}{{D_{sfl}}^2}, \frac{1}{{D_{sfr}}^2}, \frac{1}{{D_{srl}}^2}, \frac{1}{{D_{srr}}^2}\right) \tag{20}$$

4. Driving Force Distribution Method based on EMP (proposed)

Since driving force distribution method based on sum of squares minimization minimizes 2-norm, so there is a problem which differs from optimal solution min(max(λ_{ij})). Therefore, proposed EMP method which minimizes max(λ_{ij}) and has low caluculation cost is suitable to adopt driving force distribution method.

4.1. Equal Magnitude Property

By setting input as $\boldsymbol{b} \in \mathbb{R}^m$, output as $\boldsymbol{x} \in \mathbb{R}^n$, the coefficient matrix as $\boldsymbol{A} \in \mathbb{R}^{n\times m}$, the following redundant system given in (21) is the same as (16).

$$\boldsymbol{b} = \boldsymbol{A}\boldsymbol{x} \tag{21}$$

Here, this system satisfies the Equal Magnitude Property which is a property of infinity-norm as follows[8][9].

(1) There are $n-m+1$ elements that absolute values are same in the solution minimizing maximum infinity-norm.

(2) The absolute value of the $n-m+1$ elements in the theory (1) is maximum.

For applying EMP to the problem witch minimizes maximum slip ratio in straight driving, (16) is rewritten (22) using the relationship (17).

$$\begin{bmatrix} D_{sfl} & D_{sfr} & D_{srl} & D_{srr} \\ -\frac{d_f}{2}D_{sfl} & \frac{d_f}{2}D_{sfr} & -\frac{d_r}{2}D_{srl} & \frac{d_r}{2}D_{srr} \end{bmatrix} \begin{bmatrix} \lambda_{xfl} \\ \lambda_{xfr} \\ \lambda_{xrl} \\ \lambda_{xrr} \end{bmatrix} = \begin{bmatrix} F_{x\mathrm{all}} \\ M_z \end{bmatrix} \quad (22)$$

Here, to satisfy min(max(λ_{ij})), three absolute value of λ_{ij} are same. Then, these signs are same in straight driving as well as F_{xij}. Therefore, the condition of the solution which satisfies EMP is one of the follows:

$$\begin{cases} (a)\ \lambda_{fl} = \lambda_{fr} = \lambda_{rl} \\ (b)\ \lambda_{fl} = \lambda_{rl} = \lambda_{rr} \\ (c)\ \lambda_{fl} = \lambda_{fr} = \lambda_{rr} \\ (d)\ \lambda_{fr} = \lambda_{rl} = \lambda_{rr} \end{cases} \quad (23)$$

The condition of the optimal solution is (23). Thus, substituting these condition for (22), analytical solutions of each condition is obtained. That is, to identify the optimal condition from D_{sij} which represents slipperiness of the tire, optimal λ_{ij} and F_{xij} are caluculated by analytical solutions.

4.2. Deriving Condition of Optimal Driving Force Distribution

In this section, the algorithm of optimal condition which satisfies EMP, it is the condition that achieves min(max(λ_{ij})), is explaned.

In (22), the equation of yaw direction is expanded as follow. Here, since it is assumed straight driving, M_z is set zero.

$$\frac{d_f}{2}D_{sfr}\lambda_{fr} + \frac{d_r}{2}D_{srr}\lambda_{rr} = \frac{d_f}{2}D_{sfl}\lambda_{fl} + \frac{d_r}{2}D_{srl}\lambda_{rl} \quad (24)$$

To consider EMP, λ_{ij} satisfied min(max(λ_{ij})) has a relationship as follow.

$$\lambda_{km} = \lambda_{lm} = \lambda_{kn} = a \quad \lambda_{ln} = b \quad (a \geq b) \quad (25)$$

Where, subscript k, l and m, n represents front or rear, and right or left respectively.

Next, by substituting relationship (25) for (24), as it becomes $2a \geq a + b$, next D_{sij} relationship is established.

$$\frac{d_f}{2}D_{skn} + \frac{d_r}{2}D_{sln} \geq \frac{d_f}{2}D_{skm} + \frac{d_r}{2}D_{slm} \quad (26)$$

Conversely, λ_{ij} relationship as (25) is also obtained from those of D_{sij}. That is, by estimating D_{sij} and finding relationship as (26), λ_{ij} relationship which satisfies EMP as (25) can be obtained. The specific conditions is described as follows.

if

$$\frac{d_f}{2}D_{sfr} + \frac{d_r}{2}D_{srr} \geq \frac{d_f}{2}D_{sfl} + \frac{d_r}{2}D_{srl} \quad (27)$$

$$\begin{aligned} \text{then}\ \ & \lambda_{fl} = \lambda_{fr} = \lambda_{rl} = a_1 \quad \lambda_{rr} = b_1 \\ \text{or}\ \ & \lambda_{fl} = \lambda_{rl} = \lambda_{rr} = a_2 \quad \lambda_{fr} = b_2 \end{aligned}$$

else if

$$\frac{d_f}{2}D_{sfr} + \frac{d_r}{2}D_{srr} \leq \frac{d_f}{2}D_{sfl} + \frac{d_r}{2}D_{srl} \quad (28)$$

$$\begin{aligned} \text{then}\ \ & \lambda_{fl} = \lambda_{fr} = \lambda_{rr} = a_1 \quad \lambda_{rl} = b_1 \\ \text{or}\ \ & \lambda_{fr} = \lambda_{rl} = \lambda_{rr} = a_2 \quad \lambda_{fl} = b_2 \end{aligned}$$

These condition means if left wheel is slippery, λ_{ij} of both left wheels become maximum, else if right wheel is slippery, λ_{ij} of both right wheels become maximum.

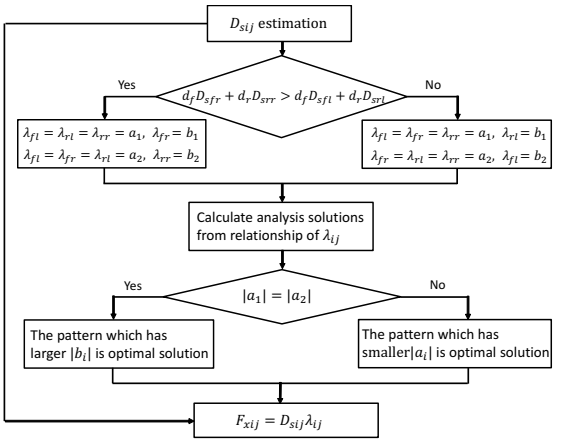

Fig. 6: The flow chart of the EMP distribution method.

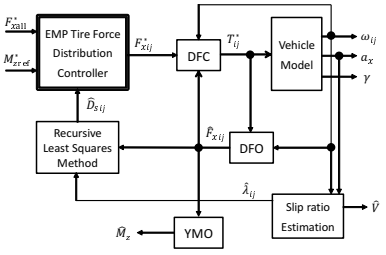

Fig. 7: The block diagram of proposal method.

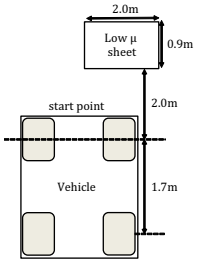

Fig. 8: Split low-μ road.

Then, about these analyzed two candidates, substituting $F_{x\mathrm{all}}$, M_z, D_{sij} for the analysis solution and caluculate λ_{ij}. After that, if two max(λ_{ij}) are different, the condition which has smaller max(λ_{ij}) is optimal, else if two max(λ_{ij}) are same, the condition which has larger min(λ_{ij}) is suitable as the optimal condition. Finally, optimal driving forces F_{xij} are calculated as estimated D_{sij} and λ_{ij} in (17).

This flowchart is described in Fig.6. By using EMP, driving forces which minimizes maximum slip ratio can be obtained with small calculate cost.

5. SIMULATION

Fig.7 shows the block diagram of the whole control system. The simulations and experiments of traction control described follows are conducted using this system.

5.1. Simulation Condition

As shown in Fig. 8, an extremely low μ ($\mu = 0.2$) surface which length is 0.9 m, shorter than the wheel base of "FPEV2-Kanon", is set at the distance of 2.0 m from the start point. The experimental vehicle starts at the start point and accelerates with total driving force reference $F_{x\mathrm{all}}{}^*$ = 2000 N and moment reference $M_z{}^* = 0$ Nm assuming straight driving. The parameters are $K_I = 0.01$, $\tau = 30$ ms, $y_{ij\max} = 0.25$ which corresponds to a slip ratio of $\lambda_{ij} = 0.2$, $\sigma = 0.5$ m/s. The wheel speed PI controller is designed by the pole assignment method towards the plant $\frac{1}{Js}$, which is from (1) ignoring F_{xij}, setting the pole -20 rad/s. The forgetting factor of the driving stiffness estimation is $w = 0.995$. All parameters are the same for each wheel.

As the conventional methods, four wheel equal distribution method and minimization sum of squares of the λ_{ij} method are simulated. As the proposed method, EMP method is simulated and compared.

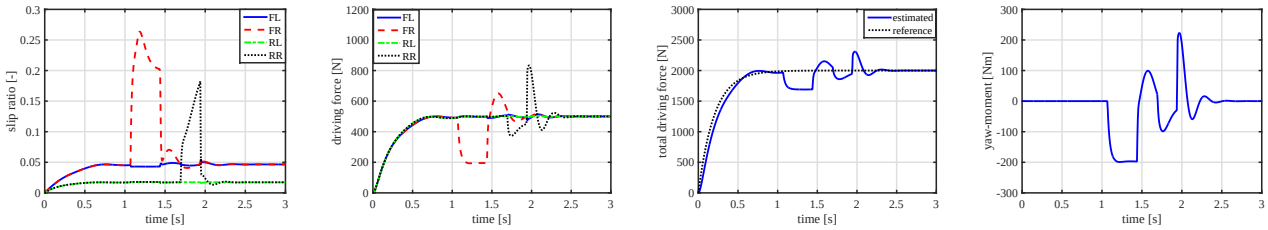

(a) Slip ratio λ_{ij} (b) Driving force F_{xij} (c) Total driving force $F_{x\mathrm{all}}$ (d) Yaw moment M_z

Fig. 9: Simulation results of instantaneous split slippery road (Equal distribution).

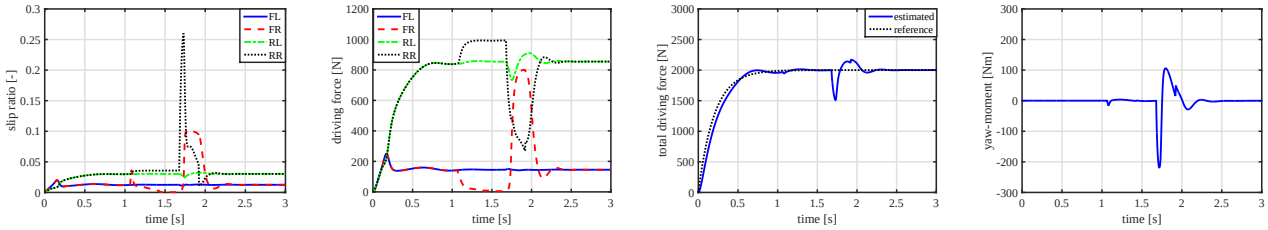

(a) Slip ratio λ_{ij} (b) Driving force F_{xij} (c) Total driving force $F_{x\mathrm{all}}$ (d) Yaw moment M_z

Fig. 10: Simulation results of instantaneous split slippery road (Minimizing 2-norm).

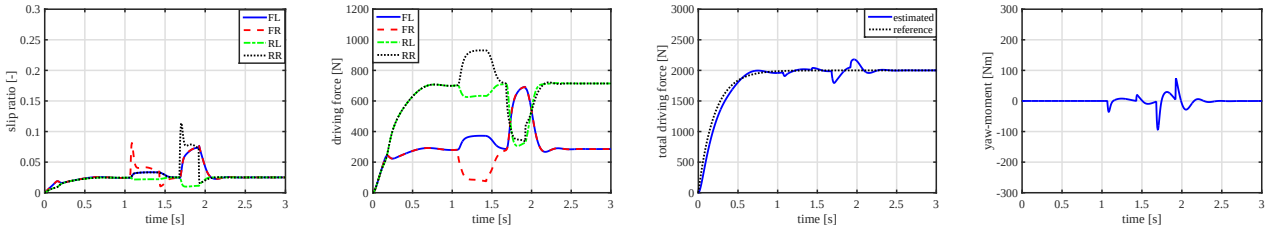

(a) Slip ratio λ_{ij} (b) Driving force F_{xij} (c) Total driving force $F_{x\mathrm{all}}$ (d) Yaw moment M_z

Fig. 11: Simulation results of instantaneous split slippery road (Proposed EMP method).

5.2. Simulation Result

Fig. 9−11 show the simulation results of acceleration test on the split slippery road.

In case of equal distribution method described in Fig. 9, driving force saturation occurs on the slippery road in Fig. 9(b), thus slip ratio rises to 0.26 in Fig. 9(a). Then total driving force couldn't be remained reference by driving force saturation Fig. 9(c) and yaw-moment is generated by driving force difference in Fig. 9(d).

In case of minimization sum of squares method described in Fig. 10, mutual complementation of driving force is achieved, but driving forces are extremely distributed in Fig. 10(b). As a result, since it couldn't be compensated decreasing of the driving force momentarily, slip ratio rise 0.26 on rear wheel in Fig. 10(a). Then, total driving force also decreases in Fig. 10(c) and yaw-moment generates momentarily in Fig. 10(d).

In case of EMP method described in Fig. 11, slip ratio is suppressed to 0.13 on the slippery road in Fig. 11(a) because driving force of slippery wheel reduces and another wheel compensates this driving force in Fig. 11(b). Therefore, the total driving force is kept as reference value in Fig. 11(c) and yaw-moment is kept zero in Fig. 11(d).

6. EXPERIMENTAL RESULTS

The Experiments are conducted under the same condition as the simulations. A polymer sheet is utilized to simulate slippery road condition. This sheet, called "low-μ sheet" in this paper, can realize a friction coefficient μ of about 0.2 by watering on it. Fig. 12−14 show the experimental results of acceleration test on the split slippery road.

In case of equal distribution method described in Fig. 12, driving force saturation occurs when the right front wheel is on the slippery road in Fig. 12(b), thus slip ratio rises to 0.25 in Fig. 12(a). Then total driving force decreases in Fig. 12(c) and yaw-moment generates in Fig. 12(d).

In case of minimization sum of squares method described in Fig. 13, since driving force is extremely distributed, it couldn't be compensated on the slippery road in Fig. 13(b). Thus, slip ratio rises 0.26 on the rear wheel in Fig. 13(a). Then, total driving force also decreases in Fig. 13(c) and yaw-moment is generated in Fig. 13(d).

In case of EMP method described in Fig. 14, slip ratio is suppressed compared with conventional methods by compensating of decreased driving force in Fig. 14(a), (b). Therefore, total driving force and yaw-moment are also kept as reference, it is found that EMP method is effective to minimize maximum slip ratio.

7. CONCLUSION

In this paper, a four-wheel driving force distribution method for minimization maximum slip ratio was proposed, its effectiveness was verified by simulations and experiments. With the proposed EMP method, slip ratios can be suppressed and the total driving force can follow the reference well. That is, stability and comfort can be achieved even on slippery roads with the proposed method.

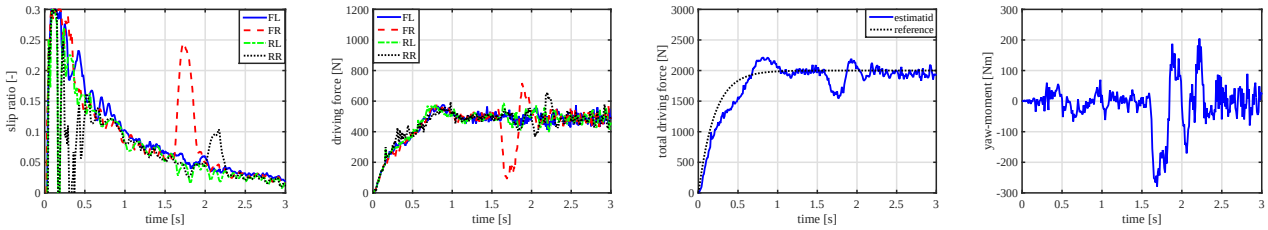

(a) Slip ratio λ_{ij} (b) Driving force F_{xij} (c) Total driving force $F_{x\mathrm{all}}$ (d) Yaw moment M_z

Fig. 12: Experimental results of instantaneous split slippery road (Equal distribution).

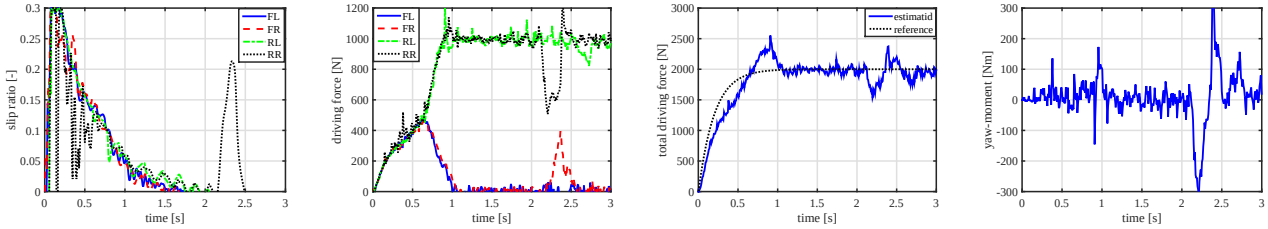

(a) Slip ratio λ_{ij} (b) Driving force F_{xij} (c) Total driving force $F_{x\mathrm{all}}$ (d) Yaw moment M_z

Fig. 13: Experimental results of instantaneous split slippery road (Minimizing 2-norm).

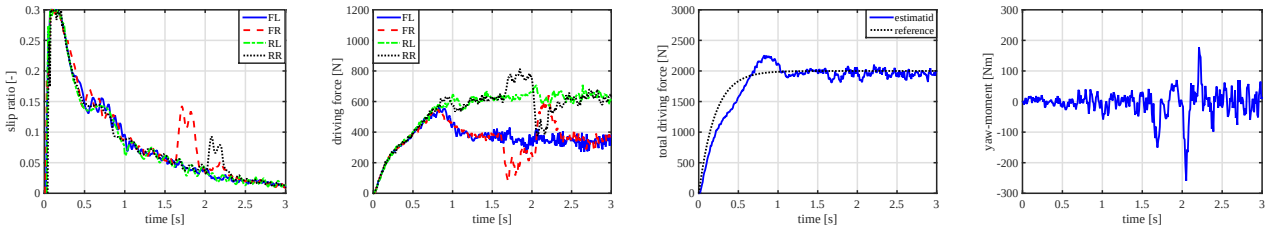

(a) Slip ratio λ_{ij} (b) Driving force F_{xij} (c) Total driving force $F_{x\mathrm{all}}$ (d) Yaw moment M_z

Fig. 14: Experimental results of instantaneous split slippery road (Proposed EMP method).

ACKNOWLEDGMENT

This research was partly supported by the Industrial Technology Research Grant Program from the New Energy and Industrial Technology Development Organization (NEDO) of Japan (No. 05A48701d), and by the Ministry of Education, Culture, Sports, Science and Technology grant (No. 22246057 and No. 26249061).

REFERENCES

(1) Y. Hori, “Future vehicle driven by electricity and control — research on four-wheel-motored “UOT Electric March II””, IEEE Trans. on Industrial Electronics, Vol. 51, No. 5, pp. 954–962 (2004).

(2) M. Yoshimura and H. Fujimoto, “Driving torque control method for electric vehicle with in-wheel motors”, IEEJ Transactions on Indstry Applications, Vol. 131, No. 5, pp. 1–8 (2010) (in Japanese).

(3) M. Kamachi, and K. Walters: “A Research of Direct Yaw-Moment Control on Slippery Road for In-Wheel Motor. Vehicle”, The 22nd International Battery, Hybrid and Fuel Cell Electric Vehicle Symposium and Exposition, Yokohama, Japan, pp. 2122–2133 (2006).

(4) H. Ogura, and T. Murakami: “Improvement of Vehicle Stability by Reaction Force Control on Accelerator Pedal and Steering Wheel”, in Proc. International Power Electronics Conference, pp. 2956–2963 (2010).

(5) O. Nishihara, and S. Higashino: “Exact Optimization of Four-Wheel Steering and Four-Wheel Independent Driving/Braking Force Distribution with Minimax Criterion of Tire Workload”, Transactions of the Japan Societ of Mechanical Engineers C, Vol. 79, No. 799, pp. 629–644, (2013). (in Japanese)

(6) O. Mokhiamar and M. Abe: “Effects of An Optimum Cooperative Chassis Control From The View Points of Tire Workload”, Proc. of JSAE 2003 Annual Congress, No. 33–03, pp. 15–20 (2003).

(7) K. Maeda, H. Fujimoto, and Y. Hori: “Four-wheel Driving-force Distribution Method for Instantaneous or Split Slippery Roads for Electric Vehicle with in-wheel motors”, 12th IEEE International Workshop on Advanced Motion Control, pp. 1–6. (2012).

(8) I. Gravagne and I. D. Walker: “Properties of Minimum Infinity-Norm Optimization Applied to Kinematically Redundant Robots”, IEEE/ASME International Conference on Intelligent Robots and Systems, pp. 152–160 (1998).

(9) Didier Quirin, Valerio Salvucci, Moto Kawanobe, Travis Baratcart, and Talafumi Koseki: “Closed form minimum infinity-norm resolution for single-degree kinematically redundant manipulators”, IECON2015–Yokohama, YF-013005 (2015).

(10) H. B. Pacejka and E. Bakker: “The magic formula tire model”, Tyre models for vehicle dynamic analysis: in Proc. the 1st Internationa lColloquium on Tire Models for Vehicle Dynamics Analysis, held in Delft, The Netherlands, pp. 1–18 (1991).

(11) T. Suzuki and H. Fujimoto: “Slip ratio estimation and regenerative brake control without detection of vehicle velocity and acceleration for electric vehicle at urgent brake-turning”, in Proceedings of the 11th IEEE International Workshop on Advanced Motion Control, pp. 273–278, (2010).